

Article citation info:

Vrublevskiy O, Napiórkowski J, Olejniczak K, Gonera J. Volumetric wear characteristics as a result of the tribological interaction between the soil with working parts cultivator's and plough's. *Eksploracja i Niezawodność – Maintenance and Reliability* 2022; 24 (4): 707–718, <http://doi.org/10.17531/ein.2022.4.11>

Volumetric wear characteristics as a result of the tribological interaction between the soil with working parts cultivator's and plough's

Indexed by:



Oleksandr Vrublevskiy^a, Jerzy Napiórkowski^a, Klaudia Olejniczak^a, Jarosław Gonera^a

^aUniversity of Warmia and Mazury in Olsztyn, Department of Vehicle and Machine Construction and Operation, ul. Oczapowskiego 11, 10-719 Olsztyn, Poland

Highlights

- An original method for analysing the local wear of operating parts materials
- Identification of the surfaces subject to intensive wear under particular conditions
- Assessment of the wear process using the local volumetric wear coefficient
- Development of a method for scanner application and validation in tribology

Abstract

This paper is concerned with the possibility of applying modern non-contact methods for assessing the wear as a result of tribological interaction between working bodies and the soil. An original method for wear testing using the test space discretization based on the 3D scanning technology was employed. A localized volumetric wear coefficient was proposed, allowing for wear analysis and improving the accuracy of the Holm-Archard model. The coefficient of local volumetric wear shows the influence of the nominal shape and the slip trajectory of the abrasive particle along the elementary surface on the intensity of wear. At local volumetric wear coefficient > 0.3 , this factor determines the intensity of surface wear. Volumetric wear characteristics are the basis for prediction of wear consequences for different materials and techniques of reinforcement of working surfaces, subject to intensive wear in abrasive soil mass. The reliability of the study is confirmed by the comparison with the mass method for wear assessment and the results of the application of the proposed method for different conditions of abrasive wear of operating parts.

Keywords

This is an open access article under the CC BY license (<https://creativecommons.org/licenses/by/4.0/>)

soil, abrasive wear, 3D scanning, operating parts, chisels, volumetric characteristics.

Nomenklature

A	cross sectional area, mm ³
F	force, N
H	hardness, N/mm ²
K_v	local volumetric wear coefficient
L	friction distance, m
l	sample length, mm
m	mass, g
S	sliding distance, mm
X, Y, Z	axis
V	volume, mm ³
v	speed, m/s

W	wear intensity, mm ³ /s
α	angle of the wedge part, °
ρ	Density, g/cm ³
Δx	one-dimensional simplex, mm
$\frac{\Delta V}{\Delta x}$	wear rate, mm ³ /mm

Indexes

i	numer of volume
f	friction
N	normal
n	nominal
w	after test

E-mail addresses: O. Vrublevskiy (ORCID: 0000-0002-5871-6381): aleksander.wroblewski@uwm.edu.pl, J. Napiórkowski (ORCID: 0000-0003-2953-7402): jerzy.napiorkowski@uwm.edu.pl, K. Olejniczak: klaudia.olejniczak@uwm.edu.pl, J. Gonera (ORCID: 0000-0001-7758-2684): jaroslaw.gonera@uwm.edu.pl

1. Introduction

It is commonly believed, both in practical and scientific terms, that the selection of appropriate construction materials helps achieve adequate operational reliability of machines. At the same time, a significant aspect associated with the analysis, i.e. the effect of varying properties of the abrasive soils mass being processed on the operating part durability depending on the operating part type, appears to be ignored. This is why the increasingly modern material solutions for operating parts proposed nowadays still result in no expected increase in durability, corresponding to the economic expenditure incurred and lead to failures and thus to machinery downtime, resulting in user dissatisfaction [15].

The operating parts that process soil mass are characterised by the highest wear intensity of all machinery parts [14]. Tribological wear, which results from friction processes leads to physical, mechanical, and chemical interactions between the surface layers of tool and machinery moving parts [22]. The properties of the surface layer of the operating part subjected to friction and the way of interaction in the tribological pair of material - abrasive environment, have an effect on the intensity of this process. The intensity of a soil-processing cutting tool wear is determined by the abrasive soil mass properties, the operating part's characteristics, and the interaction mechanics occurring in the tribological pair [19, 20]. The rate of these changes is determined by randomly varying environmental conditions.

Steels have been, and in most cases will remain, the main construction material for operating parts to process a soil mass. On the one hand, this is due to the relationship between manufacturing costs and the durability of wear-resistant materials, while on the other, to the versatility of use, good weldability, ease of machining and their constantly improving mechanical properties [13, 17]. Based on the available literature, it can be concluded that the topic of operating parts' wear in the soil is still relevant, which is reflected in the large number of published scientific papers. In particular, they present the possibilities for increasing the durability of these parts by using materials with increased resistance to abrasive wear with specific chemical and mechanical properties. In addition to hard faced materials, alloy and micro-alloyed steels with the addition of niobium and boron are dominant among them [4, 7]. The available literature includes scientific papers on the modification of the chemical composition of boron steel, or on the application of specific thermo-plastic processing conditions to their manufacture in order to obtain the required functional properties [12].

Although the issue of intensive wear in an abrasive soil mass concerns many industrial sectors, the results most often presented in the literature are those of research in the field of agricultural technology. Yazici [24] conducted a study on the reduction in wear of ploughshares manufactured by hot stamping and hardfacing. According to his study results, hot stamping and hardfacing with C-Cr-based alloys can be recommended as an effective solution to reduce ploughshare wear. A paper by Bayhan [3] presents a study into increasing wear resistance by coating ploughshare chisels manufactured from low-alloy steels with three different hardfacing electrodes designated EH-600, EH-350, and EH-14Mn. The study noted statistically significant differences in wear intensity under laboratory and field conditions. Having taken costs into account, it was concluded that hardfacing with the EH-600 and EH-350 electrodes had a measurable economic effect. Horvat et al. [10] presented a comparison of the wear of mouldboards and two ploughshares manufactured from different materials and hardfaced by the SMAW process. The change in geometry and the weight loss were smaller for both hardfaced ploughshare types as compared to the original ploughshare. A study by Bialobrzaska and Kostencki [5] compared the results of ploughshare wear tests by the field method with those obtained by the laboratory method for selected low-alloy steels with the addition of boron. They conducted both field and laboratory tests to determine the highest and lowest resistance to abrasive wear. Napiórkowski et

al. [18] demonstrated that abrasive wear resistance of silicon carbide was determined by the particle size distribution in the soil being processed. Silicon carbide achieved the highest resistance in a light soil. The hardfaced layer exhibited higher abrasion resistance under different soil conditions. Silicon carbide on the nitride bond exhibited higher abrasion resistance than that of the analysed boron steels in all soil types.

A commonly applied method for assessing wear is the determination of weight loss and the change in linear dimensions of the operating part [5, 10, 24]. Due to the different weights of parts and, thus, their different friction surface area, weight wear should be used when assessing the wear of parts of an identical design. For working elements composed of heterogeneous materials, the use of the mass method is not reliable. The progressive digitisation of surface condition monitoring processes, and the continuous development of tribological research create a demand for the development of methods for verifying changes not only in the surfaces involved in friction processes but also in the operating part's geometry.

Vrublevskiy et al. [23] proposes a new approach analysis of changes in the shape of a working component of an agricultural machine. For this purpose, chisels of ploughshares used under varied soil conditions were analyzed. Numerical models of worn-out working parts created using 3D scanning were the basis for developing.

Using wear models, it is possible to forecast the rate of material loss from a given element. The classic theory of wear assumes that the assessment of the wear process begins with the identification of the hardness of the material, the intensity of material removal, the given load and the probability of the material removing the wear particle at a given contact moment [1, 2]. There are three main trends in model development. The first is based on empirical equations, the second is a mechanical approach, and the last is based on material. However, no generalization has been achieved with regard to consumption at any level. Meng [16] discovered during his research that 100 parameters were used in total in over 180 models. Important in the work [16] is the conclusion that in most works that volumetric changes in the working body are the main characteristic of the change in the functional properties of the working body and the main characteristic of wear for all models.

The first successful attempts have also been made to use 3D scanning to assess the wear process. Cucinotta et al. [6] applied 3D scanning to identify the wear of the cutting surface of the ploughshares mounted on four bodies of a soil-processing plough. They also presented a method for the development of a digital model of worn surfaces. Their study identified differences in volume losses and changes in the profile of the cutting edge between ploughshares depending on the mounting location. The literature also includes studies that present changes in the volume and shape of operating parts used in manufacturing automotive parts. Hawruluk et al. [8] conducted a study that enabled the determination, using 3D scanning, of the wear of forging dies used for manufacturing motor valves. The forging dies were tested in cycles, after a specified number of valves were manufactured. The losses in production tool material were determined, and the quality and changes in the geometry of the forging die surface layer were directly monitored. The study [9] also addressed the issue of forging tool wear. Following the performance of 3D scanning, an analysis of the tool wear course was conducted. Changes in volume in selected areas of forgings were determined following the forging of an appropriate number of components. Periodic tests enabled the identification of wear over time in relation to the reference model. For the scanning, an integral scanning system with an accuracy of 0.035 mm was used in accordance with ASME B89.4.22. The area testing method proposed by the authors does not analyse changes in the wear volume. The identification of the extent of wear of machinery operating parts using 3D scanning enables the determination of the tool wear limit value beyond which the processing of the material is already affected by defects and deteriorates the product quality [25]. An analogous problem is encountered when processing soil, e.g. in ploughing processes,

yet the wear is caused by different factors. The wear of tool operating parts results in increased energy consumption, decreased productivity and deteriorated process quality. Ranusa et al. [21] used a 3D scanner to identify the wear of hip prostheses. The authors compared the wear of parts periodically, following the performance of specified work using nominal parts. The studies considered the number of samples, process duration and the friction distance, while it is difficult to find studies into changes in volume in relation to changes in the geometry. In the current state of knowledge, it is important to select the appropriate material for parts that will undergo the least wear and ensure increased durability. The literature review shows that the wear volume can be determined, e.g. using the Holm-Archard model – in which the wear volume is determined by an indirect method from linear measurements [17]. This method, involving the determination of volume based on the measurements of the mass, is of limited accuracy due to the use of materials with varying densities.

When conducting research, much attention is paid to linking changes in the geometry of an operating part with the way it gets worn. What is particularly important in the identification of geometry changes is the cutting edge shape which most often determines whether the part reaches its limit state. The assessment of changes in the operating part shape is possible through a three-dimensional approach to the problem. Obtaining volumetric changes in the geometry of an operating part provides the basis for developing a digital spatial model. The application of volumetric characteristics will enable the identification of the most complex changes in the shape of operating parts and provide the basis for the elimination of changes in the part weight from the assessment of wear.

The aim of the study is to develop volumetric characteristics of the operating part wear process in an abrasive soil mass. Solving this problem will allow changes in the wear area to be studied not on a macro- but on a micro-scale, and the factors affecting local wear to be identified.

The study results are provided in the following order: Section 2 presents the materials and the methodology for volumetric wear testing. Section 3 presents the study results, and compares the mass method with the volumetric method. The analysis of the obtained wear characteristics is presented in Section 4. In the Conclusions, the obtained results are discussed, and the direction of further research is indicated.

2. Methodology of the study

The development of the volumetric wear characteristics and the prediction of wear required several test stages in a specific sequence (Fig. 1). First, a 3D scan of the nominal elements was performed. Subsequently, these elements were subjected to tribological tests, which were actually operational testings. During the tests, the decisive parameter was the type of soil and the amount of work performed. After this stage of the research was completed, the surface microstructure was assessed and the worn parts were 3D scanned. Based on the comparison of the 3D surfaces of the worn and nominal elements, the total volume of the used material was determined, as well as the elementary volumes of the test objects after discretization of the model. In addition, a verification was carried out to identify differences in consumption between the volumetric and mass methods.

Based on the obtained data, new volumetric wear characteristics and a method of predicting volumetric wear of working elements were proposed.

2.1. Material

The volumetric characteristics obtained as a result of the use of 3D scanning technology proposed in the work can be used to assess the wear of elements with a complex shape and elements consisting of zones of different density. The samples selected for the tests constituted the physical model. The chisels, on the other hand, are the actual working element of the plow for tilling the soil.

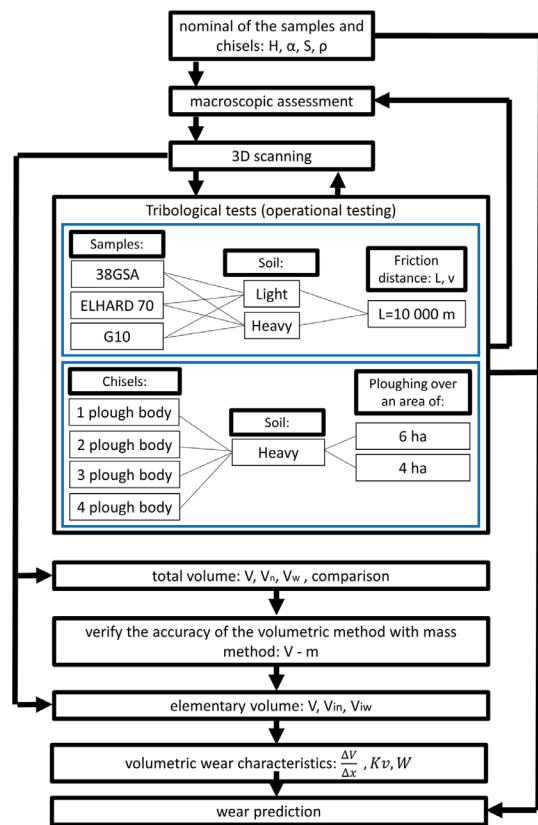


Fig. 1. Diagram of tests performed at work

In the first stage, the test material comprised samples made from 38GSA steel, padding weld EL HARD70, and sintered tungsten carbide G10 applied onto 38GSA steel. The nominal dimensions and shape of samples are provided in Fig. 2.

The measurements of test material hardness were conducted by the Vickers method under conditions compliant with standard PN-EN ISO 6507-1:1999. The measurements were conducted using a Zwick 32 hardness tester with a load of 9.807 N operating for 15 s. The chemical composition (Table 1) was analysed by the spectral method using a Leco GDS500A glow discharge emission analyser, with the following parameters applied: U = 1250 V, I = 45 mA, argon. For the light microscopy testing, a Zeiss Neophot 52 microscope coupled with a Visitron Systems digital camera was used. The scanning electron microscopy (SEM) testing was conducted using a JEOL JSM-5800 LV scanning microscope coupled with an Oxford LINK ISIS-300 X-ray mini-analyser. For the macroscopic assessment of the surfaces following friction tests, a KEYENCE VHX-6000 digital microscope was used.

The microstructure of the chisels was assessed using the Phnom XL scanning electron microscope. The microscope was compressed with an X-ray microanalyzer. Using the installed BSD, SEM and EDS detectors, it was possible to obtain information about the topography and chemical composition of the analyzed surface. Evaluation of the microstructure was carried out in the material contrast. Nital 5% was used to etch the chisels prior to microscopic observation. The chemical composition was assessed with the Thermo ARL Quantris spark spectrometer using the CCD technique.

The samples (Fig. 3) from low-alloy martensitic steel 38GSA were acquired directly from a steel plant. The steel was manufactured using hot rolling technology and subjected to normalisation under metallurgical conditions in order to break down the microstructure. The average hardness of the steel was 420 HV10. The microstructure comprised fine dispersed perlite with ferrite and martensite grains.

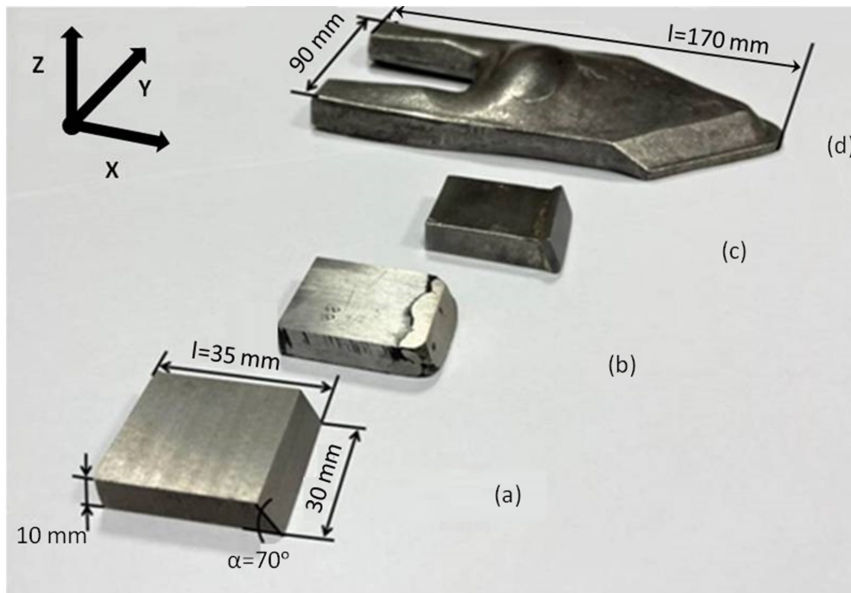


Fig. 2. The appearance of test materials: (a) steel 38GSA; (b) padding weld ELHARD70; (c) specimen with sintered carbide G10; (d) knock-on chisel

The Elhard 70 electrode (Fig. 4) was applied onto 38GSA steel. The padding weld had a ledeburite structure with large precipitates of primary chromium carbides and a few small-sized boron carbides. The padding weld hardness at the 5 mm thickness ranged from 674 HV10 (on the surface) to 871 HV10 (at a 3 mm depth).

The third material (Fig. 5) comprised samples made from 38GSA steel with sintered tungsten carbide G10 plates soldered on it. The structure comprised α - initial tungsten carbide (WC) with a particle size ranging from 0.001 to 0.002, and $\alpha 1$ - a solid cobalt solution in the initial tungsten carbide (WC) that did not re-crystallise during sintering. The highest hardness measured on the carbide surface was 1423 HV10.

The operational testing was conducted on 80 mm knock-on chisels (Fig. 6). The system was developed to improve the plough's penetration ability, stabilise it, and maintain the pre-set cutting depth. The chisels were manufactured from boron steel with a martensitic structure and post-martensitic orientation, with very few carbide phase precipitates inside the martensite laths. The average hardness of the surface

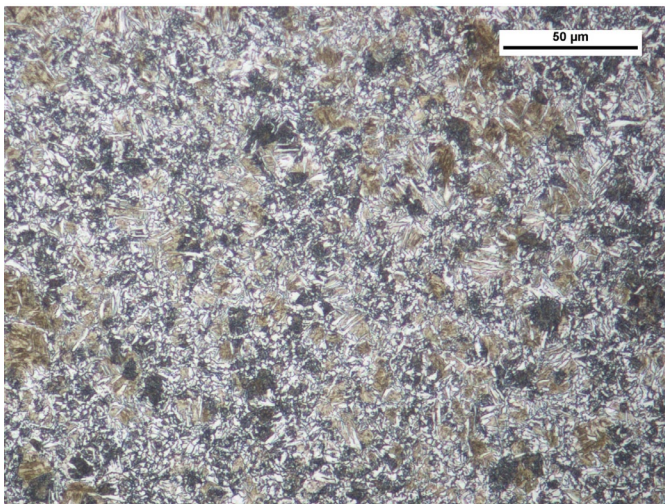


Fig. 3. Microstructure of fine-dispersion perlite with ferrite grains and martensite precipitates of 38GSA steel in the delivered condition; Magnification 500x, etched with 3% HNO₃ (Mi1Fe), light microscopy

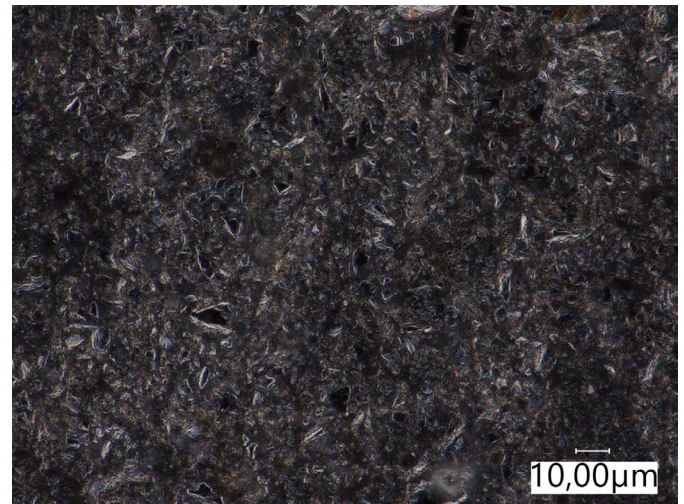


Fig. 5. Microstructure of the cemented carbide G10

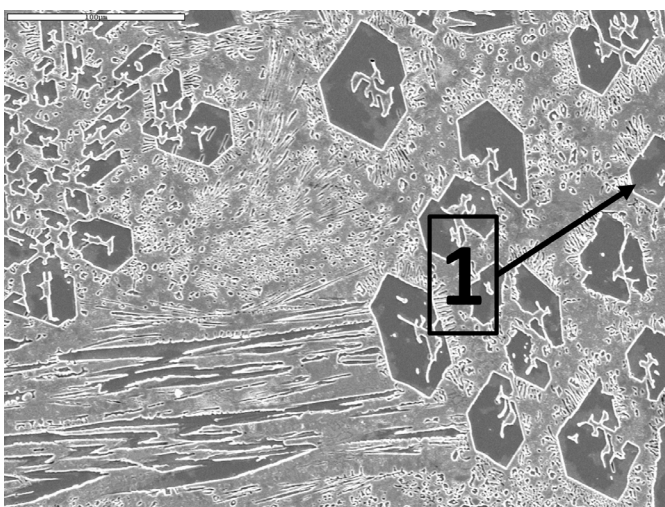


Fig. 4. Microstructure of the padded layer. Large, primary precipitates of chromium carbides (1) in the matrix of the mixture of alloy ferrite and carbides. Magnification 350x, etched with 3% HNO₃ (Mi1Fe) and then electrolytically with chromic acid, SEM

layer was 560 HV. The nominal dimensions are presented in Fig. 1d, while their weight was 1000±5 g. Chisels of this type were mounted on the ploughshare using a dedicated holder.

2.2. Tribological tests

The operational testing of samples were conducted under the actual operational conditions in two soil types: heavy loam (designated as a heavy soil) and loamy sand (designated as a light soil). The light soil is an extremely abrasive soil, because to the high content of sand. The samples (Figs. 2a-c) were mounted on a 9-tined cultivator with spring tines, aggregated with an agricultural tractor (Fig. 7a). The samples were operated when the cultivator was operating at a depth of 0.12 m. Along the friction path equal to 5 km, the order of mounting the samples in the cultivator was changed. The average speed of the unit was 1.9 m/s, while the friction distance was 10 000 m. The soil moisture ranged from 12% for the light soil to 15% for the heavy clay, which corresponds to moist soil. The particle size distribution was tested by the laser diffraction method using a Mastersizer 2000 laser particle composition meter in accordance with standard ISO 13320 (Table 2).

The operational testing of chisel wear was conducted while ploughing at a depth of 0.25 m using a John Deere 6930 agricultural tractor with an ES 100 four-bodied reversible plough (Fig. 7b). The average tractor speed was 1.9 m/s, 8 chisels were tested. Two chisel sets were

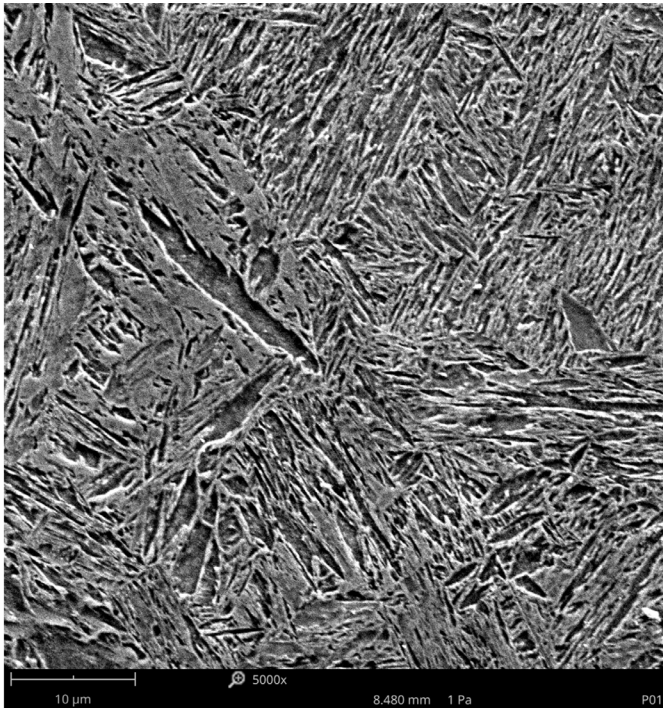
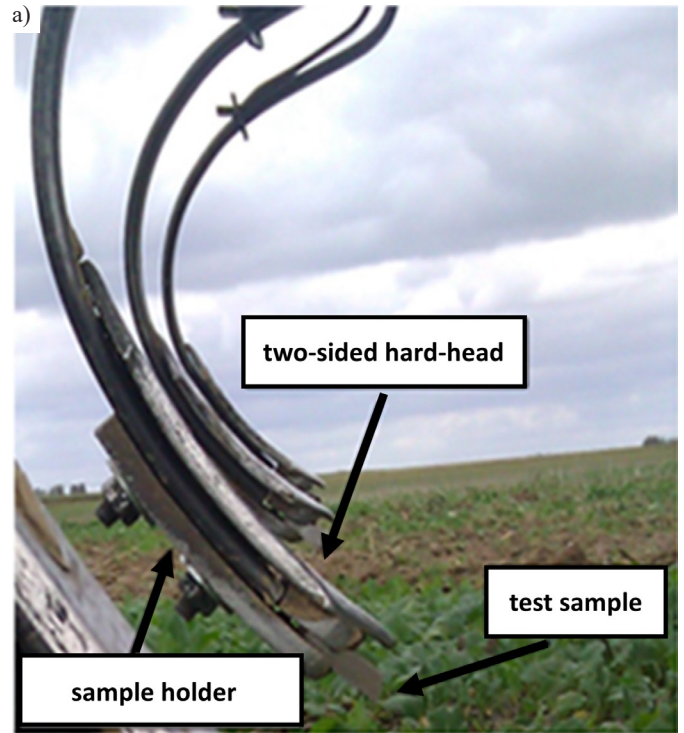


Fig. 6. Microstructure of boron steel in chisels



used for the operational testing. The first set carried out ploughing over an area of 6 ha, while the other over the area of 4 ha. The way the chisels were mounted is presented in Fig. 6b. The chisel designated with number 1 was mounted on the first body (closest to the tractor). The chisel wear tests were only conducted in heavy soil.

The weight of the test objects was measured using an AXIS B2000 balance with an accuracy of 0.1 g. For each material under specific conditions, tests were carried out with the use of five samples in order to increase the accuracy and determine the measurement error.

2.3. 3D scanning

Prior to the tribological testing of the analysed samples and chisels within an abrasive soil mass, the nominal geometry of the study subjects was scanned. To this end, an



Fig. 7. Method of mounting: (a) a specimen in the holder; (b) a chisel

Table 1. The chemical composition of the tested materials.

Material	[% mass.]									Hardness [N/mm ²]	Density [g/cm ³]	Metallurgical structure
	C	Cr	Mn	S	Al	B	Mo	WC	Co			
Martensitic steel 38GSA	0.35	1.17	1.07	1.17	0.022	-	-	-	-	420	7.80	fine-dispersion perlite with ferrite grains and martensite precipitates
Padding EL-HARD70	5.0	38.0	-	-	-	3.5	-	-	-	871	6.2-6.9	large, primary precipitates of chromium carbides in the matrix of the mixture of alloy ferrite and carbides
Tungsten carbide G10	-	-	-	-	-	-	-	94	6	1423	14.8	initial tungsten carbide and a solid cobalt solution in the initial tungsten carbide that did not recrystallise during sintering
Chisels made of boron steel	0.3	1.02	1.25	1.02	0.04	0.002	0.01	-	-	560	7.65	boron steel with a martensitic structure and post-martensitic orientation, with very few carbide phase precipitates inside the martensite laths

Table 2 Characteristics of the particle size distribution in an abrasive soil mass

Granulometric groups	Fraction diameter [mm]	Fraction content [%]	
SAND	2.0 – 0.05	33.62	77.06
SILT	0.05 – 0.002	49.92	21.37
CLAY	< 0.002	16.56	1.57
Determination according to PTG 2008		heavy soil	light soil

Atos Core optical 3D scanner with an accuracy of 0.02 mm, and the GOM Inspect® software were used. The scanner had a projector with a structural blue light and two cameras. The scanning (Fig. 8) of a single part required, depending on its size, between several (for the samples) and several dozen (for the chisels) individual scans to be taken, which were subsequently combined using the markers placed on the part being scanned. During the scanning, a point cloud was obtained from the surfaces of the analysed objects (triangulation). Subsequently, a 3D model was generated, from which a triangle network was prepared to obtain an STL model. The developed nominal specimen and chisel models were compared to corresponding models of worn operating parts within an abrasive soil's mass depending on the specimen type, soil conditions and the place where the chisel was mounted on a four-bodied reversible plough.



Fig. 8. The process of 3D scanning of: a) specimen; b) chisel

2.4. Volumetric characteristics

In order to obtain integral and differential volumetric characteristics of wear, the specimen was divided into elementary volumes. This

division can be based on evenly distributed planes parallel to each other. The location of the plane in relation to the surface being worn can be determined by the specimen's longitudinal coordinate (Fig. 9).

The volumes ΔV_{in} (nominal) and ΔV_{iw} (after test), contained between the adjacent planes I and II, enable the determination of the volume ΔV_i of the worn material as $\Delta V_i = \Delta V_{in} - \Delta V_{iw}$. With a $\Delta x = 1$ mm distance between the planes, the volumetric wear unit was mm^3/mm .

Then, the total volume V of the worn material was determined as:

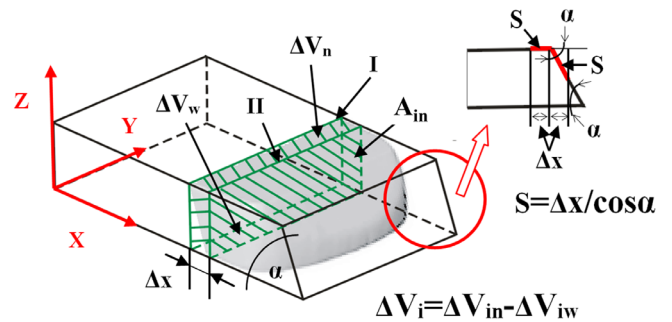


Fig. 9. The formation of elementary volumes on test specimen

$$V = \sum_{i=0}^l (\Delta V_{in} - \Delta V_{iw}), \quad (1)$$

where l is the specimen length (Fig. 1).

With the volume of the worn material, it was possible to determine the local volumetric wear coefficient K_{vi} , as a relationship between the $\Delta V_i/\Delta x$ ratio and the nominal cross sectional area A_{in} (Fig. 9) in the area under consideration:

$$K_{vi} = \frac{\Delta V_i}{\Delta x} \cdot \frac{1}{A_{in}}. \quad (2)$$

The local wear coefficient defines the share of wear in the nominal elemental volume, taking into account the displacement path of the abrasive particle along the working surface. Equation (2) contains the $\Delta V_i/\Delta x$ ratio, which determines the volumetric wear rate. It is proposed that the volumetric wear rate should be defined as the ratio of the volume of the material used to the one-dimensional simplex, which determines the boundaries of the working surface under consideration. For a flat nominal surface, and assuming that the X-axis direction determines the movement of soil particles over the prismatic surface, the Δx value can be defined as the sliding distance S of a soil particle over the surface. Having considered the location of wear, the $\Delta V_i/\Delta x$ ratio has a definition similar to that used in the well-known Holm-Archard's expression: $\frac{V}{L} = K \cdot \frac{F_N}{H}$ [11]:

$$\frac{V}{L} = K \cdot \frac{F_N}{H} \quad (3)$$

where: V - wear volume [mm^3], load F_N [N], friction distance L [m], wear coefficient K [-], and material hardness H [N/m^2].

Obviously, with a wedge-shaped work surface, the particle's sliding distance will be longer than Δx . In order to take into account of the trajectory of particle's movement over a wedge-shaped surface with

an α angle (Fig. 9), equation (2) should be presented in the following form:

$$K_{vi} = \frac{\Delta V_i}{S \cdot \bar{\epsilon} \cos \alpha} \cdot \frac{1}{A_{i \bar{n}}}, \text{ where } \begin{cases} \alpha = 0^\circ \text{ without a wedge} \\ \alpha < 90^\circ \text{ wedge} \end{cases} \quad (4)$$

Then, for the elementary nominal volume from equations (3, 4), the normal load F_N can be presented as follows:

$$F_{Ni} = H_i \cdot \frac{K_{vi} \cdot S \cdot \bar{\epsilon} \cos \alpha}{K \cdot L} \cdot A_{i \bar{n}} \quad (5)$$

Equation (5) enables the estimation of the load leading to a reduction in the worn volume of an operating part due to abrasive wear. The relationship takes into account the material properties (hardness), the surface geometry (volumetric wear coefficient and the cross sectional area of the operating part), and the surface quality (soil movement trajectory).

Wear models, e.g. equation 3, are often used to prediction the worn material volume. Therefore, the wear volume is the subject of direct measurement using 3D scanning technology.

3. Study results

After tribological tests, the surfaces of test materials were analysed in order to identify the ways they were worn under different soil conditions. When the materials were being worn in the light soil, the loosely bound abrasive particles, characterised by high freedom of movement, caused scratching and ridging on the friction surface (Fig. 10). As the fine fractions in the soil mass increased, the process of their penetration into the discontinuities of the surface layer occurred. Hence, there are numerous scratches and sand particle residues on the surface of the material being worn in the light soil. In the few cases when the possibility of movement was limited, micro-cutting took place, which resulted in chipping off the layer. It indicates that sand grains interact with the surface in a discrete manner. Only for the material from

sintered carbide G10, the surface is slightly scratched and the wear processes are hardly noticeable.

As the content of loam and dust particles in the soil increases, a different course of wear can be noted (Fig. 11). The sand fraction comprises solely quartz SiO_2 . Dust and silt fractions contain mostly compounds of amorphous silica and silty minerals. The impact of silt and clay alone is negligible, but it intensifies when they are in combination with other fractions. When humid, these fractions act like an adhesive for quartz. Fatigue wear is evidenced by local surface tearing out resulting from multi-cycle wear, which includes elastic deformation, plastic deformations, the formation of micro-volume threshold strains characterised by a defective structure and the cutting of these micro-volumes. Numerous dents in the surface are filled with the abrasive mixture, owing to which SiO_2 grains have fewer degrees of freedom, therefore the share of sliding friction increases at the expense of rolling friction. The process in question is the wear caused by reinforced abrasive grains. The nature of wear changes, which results in its increased value.

When identifying the operating part wear values, the method described in subsections 2.3 and 2.4 was employed.

The cross sections were made along the X-axis (Fig. 12). The first cross section was located at a distance of 20 mm from the initial part of the chisel since no wear of the surface was noted up to a distance of 20 mm (the area where the chisel was mounted on the ploughshare). The second cross section was made at a distance of 69 mm. From the distance of 69 mm onwards, the cross sections were made at 5 mm intervals, as it was an area of accelerated wear of the chisel surfaces that varied depending on where the chisel was mounted on the four-bodied reversible plough. The greatest number of cross sections were made for chisels mounted on the fourth body due to the least wear.

In order to verify the accuracy of the 3D scanning method, measurements of both nominal and worn chisels or samples were conducted. The mass wear being measured (Table 3 and Table 4) was compared with the mass wear calculated based on the measurements of chisels or samples volumes obtained from scanning. The measurement results and the comparison are presented in Table 3 and Table 4, where: m_M – chisels or samples weight loss, V – the volume of chisels or samples

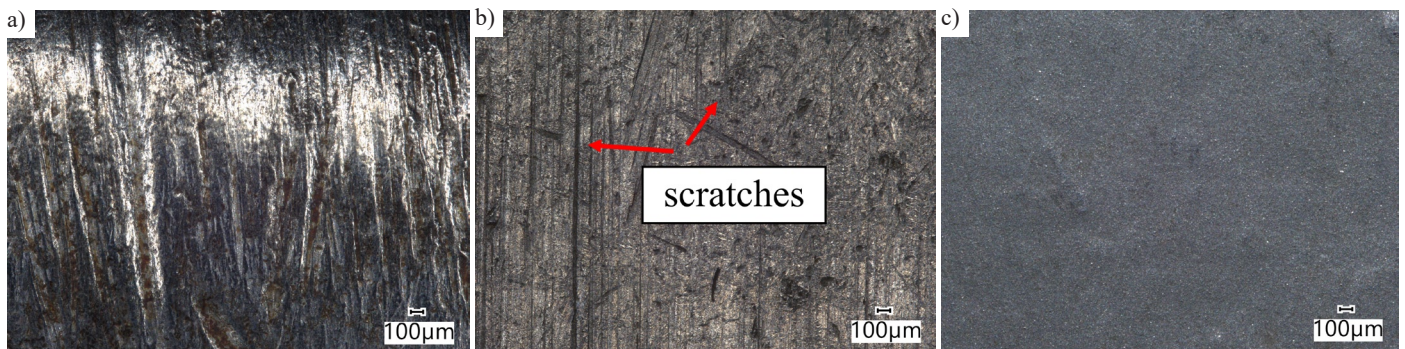


Fig. 10. The appearance of specimen surface after being worn in a light soil: (a) 38GSA steel; (b) ELHARD70; (c) sintered carbide G10

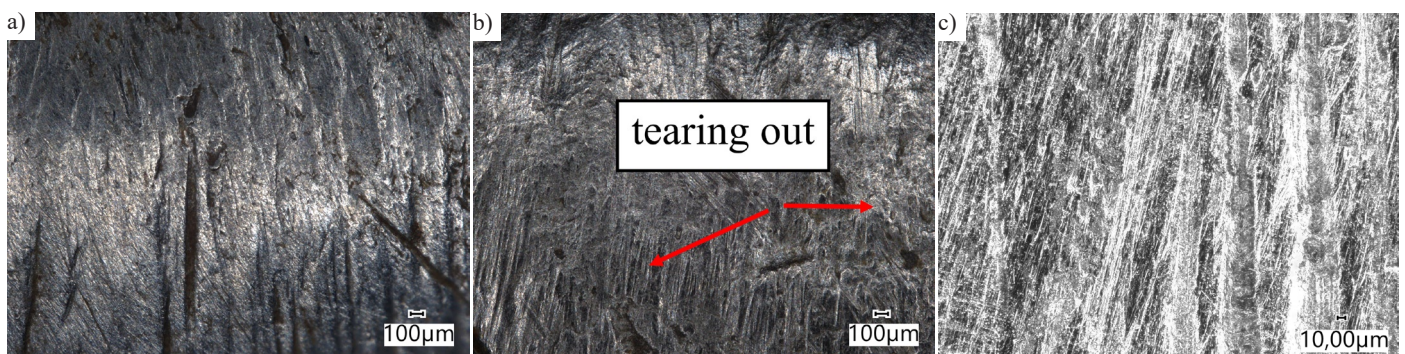


Fig. 11. The appearance of the specimen surface after being worn in a heavy soil: (a) 38GSA steel; (b) ELHARD70; (c) chisel

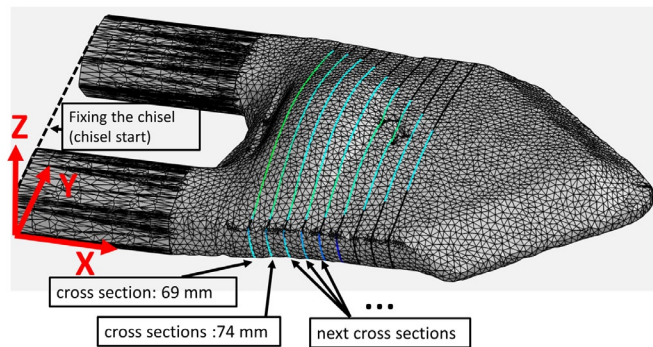


Fig. 12. Cross sections made along the X-axis

wear obtained from the 3D scanning process (eq. 1), m_v – chisels or samples weight loss determined based on the scanning results.

Similarly, the verification of the proposed method was carried out by measuring the weights of nominal and worn samples (Table 3) as well as chisels (Table 4).

The differences between the measured weight loss and the weight determined by the volumetric method as a result of scanning (Δm) reach a maximum value of 1 g, which accounts for approx. 0.2% of the chisel's total weight. Such a negligible difference is indicative of the good accuracy of the applied 3D scanning method for the purpose of chisel volume determination.

An additional advantage of 3D scanning is the possibility for distinguishing the operating part's volume (Fig. 13), which enables detailed examination of local wear and the areas of operating part rein-

Table 3. Results of the specimen wear determination by the volumetric and mass methods.

	heavy soil			light soil		
	volumetric method (V)		mass method (M)	volumetric method (V)		mass method (M)
	V	m_v	m_M	V	m_v	m_M
	mm^3	g	g	mm^3	g	g
38GSA	3836.91	29.93	29.2	849.3	6.62	6.1
ELHARD70	1404.31	10.72	11.6	616	4.59	5.6
Tungsten carbide G10	805.28	6.52	6.7	286.117	2.31	2.6

Table 4. Results of the chisel wear determination by the volumetric and mass methods.

	volumetric method (V)		mass method (M)	$\Delta m = m_M - m_v$ [g]	
	V	m_v	m_M		
Chisel No	mm^3	g	g		
6 ha	1	91329.34	698.9	698.7	-0.2
	2	82779.55	633.4	633.3	-0.1
	3	77214.68	590.8	591.1	0.3
	4	65766.30	503.2	504.0	0.8
4 ha	1	86736.96	663.7	663.8	0.1
	2	76278.64	583.7	584.0	0.3
	3	71001.02	543.3	543.4	0.1
	4	65158.89	498.6	499.6	1.0

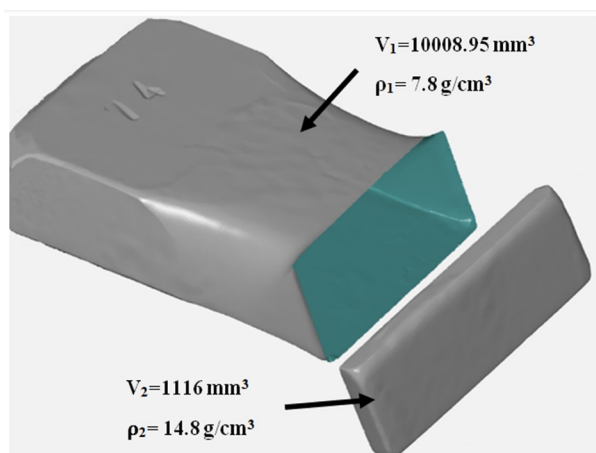


Fig. 13. The division of volumes for the specimen with sintered carbide G10: (a) 3D scan; (b) the actual specimen with sintered carbide G10

forcement (with the least wear). Local reinforcement is a priority in increasing the operating parts' resistance to abrasive wear. Following the scanning, the volume of G10 carbide with an almost doubled density can be distinguished. Not only the material but also the shape of the operating part can determine the volume diversity.

4. Result analysis and discussion

On the example of a sample made of 38GSA steel and used in heavy soil, the accuracy of K_{vi} determination in the area of intensive wear was ± 0.07 (Fig. 14), while in the area with lower wear intensity, the standard deviation was ± 0.025 . On the basis of five samples, the average value of the measurements was obtained, presented in Figures 15 and 16. For the remaining materials, the consumption was also analyzed on the basis of measurements made for five samples of a given type and in two soil conditions. The average values of wear and standard deviation were lower than for the described sample.

In order to determine the influence of the cross section distance from the beginning of the sample (sample length = 0 mm) on change in the K_{vi} coefficient, the analysis of variance was used. For each of the tested samples, the null hypothesis about the lack of differences between the coefficient values and the alternative hypothesis about the existence of significant differences in the coefficient changes was adopted.

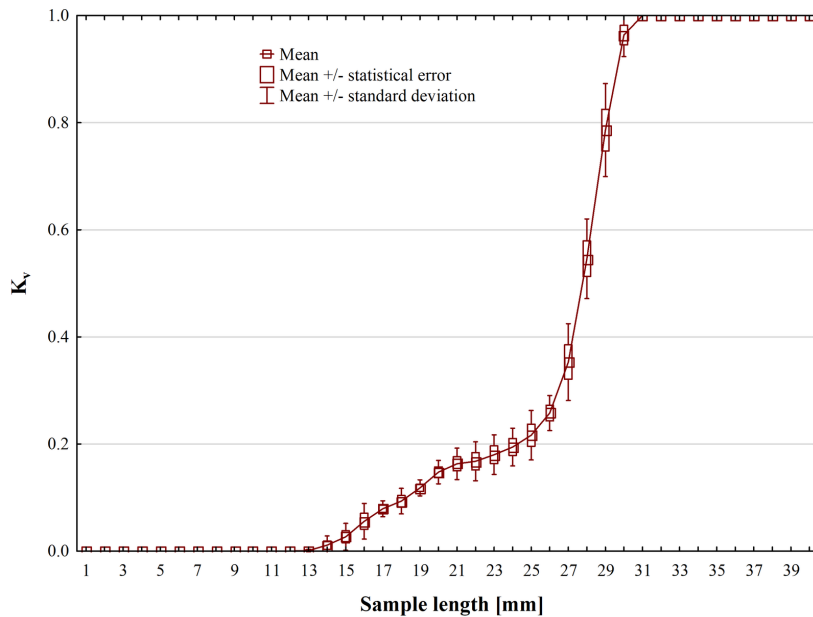


Fig. 14. Characteristics of local volumetric wear of 38GSA steel samples (heavy soil)

On the basis of the collected data, it can be observed that between the individual cross sections there were significant differences in the value of the K_{vi} coefficient in the area of intense wear (sample length over 26 mm).

Characteristics K_{vi} vary depending on the materials and the technology of producing the samples shown in Fig. 2. If a specimen is of a regular shape, the change in wear volume is linear. A change in the shape is defined as a deviation from the linearity of an increase/decrease in the local wear. This can be explained by the change in the direction of the nominal and friction force, and the time of contact between the abrasive particles and the surface that shapes the elementary volume ΔV_{iv} . For example, samples from 38GSA steel are character-

ised by a transition from a prismatic wedge surface to a parallelogram surface. It is at the transition point that the change in wear intensity along the specimen length can be observed. The characteristics of the specimen with a padding weld exhibit similar properties (Fig. 15).

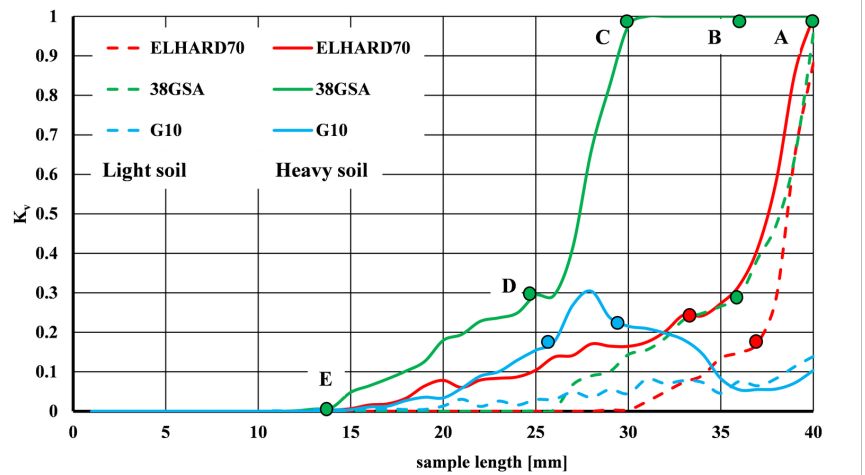


Fig. 15. Characteristics of local volumetric wear of samples (Figs. 1a-c)

A slightly different nature of the wear location is observed for samples reinforced on the front side of the operating surface with sintered carbide G10 (Fig. 16). For this solution, the wear of the specimen's front part is significantly reduced. The intensive wear of 38GSA steel on the prismatic surface results in a local increase in the linear trajectory S of the abrasive particle $S > \Delta x$. At $K_{vi} > 0.3$, this factor determines the intensity of surface wear.

The description of the wear process results using the volumes enables a more detailed study into not only selected elementary volumes but also the surfaces forming these volumes. For example, the front and side surfaces can be selected. In this case, the shape changes the most on the side surfaces. Possible main reason for this is the way the nominal force F_N and the friction force F_f operate, and the particles' movement trajectory. On the front surface of the soil-attacking specimen, the friction coefficient value drops due to the inequality $F_N > F_f$, where: F_f is friction force. For example, for ΔV_{24w} , the total ratio is 41.125 mm^3 . On the side surfaces, the wear is 26.125 mm^3 , which accounts for 63.52% of the ΔV_{24w} value.

The characteristics presented in Fig. 17 can be used to determine the friction path L , at which the total wear of the elementary part of the sample ΔV_i occurs. For this purpose, after the predetermined friction path ($L = 10000 \text{ m}$) at the time of scanning the samples at the speed ($v = 1.9 \text{ m/s}$) of the sample displacement during the tribological test, the wear intensity for the volume ΔV_i can be determined. The wear intensity will be determined as $W = \Delta V_i / vL$. The volumetric wear intensity determines the ratio of the elementary volume of the material used to the unit of work time performed when cutting the soil. Consequently, at point C (Fig. 15) the wear intensity W will be maximum and will amount to $4.5 \cdot 10^{-5} \text{ mm}^3/\text{s}$. In the section ABC wear intensity $W = 1.55 \cdot 10^{-4} \text{ mm}^3/\text{s}$, which enables the determination of the friction distance L up to the complete consumption of the samples. The total wear of the first elementary section of the sample (closest to the working edge) will take place after the friction path L of 364.67 m has been traversed. However, the total wear of the specimen wedge surface will take place after the friction path of 4360.88 m has been traversed.

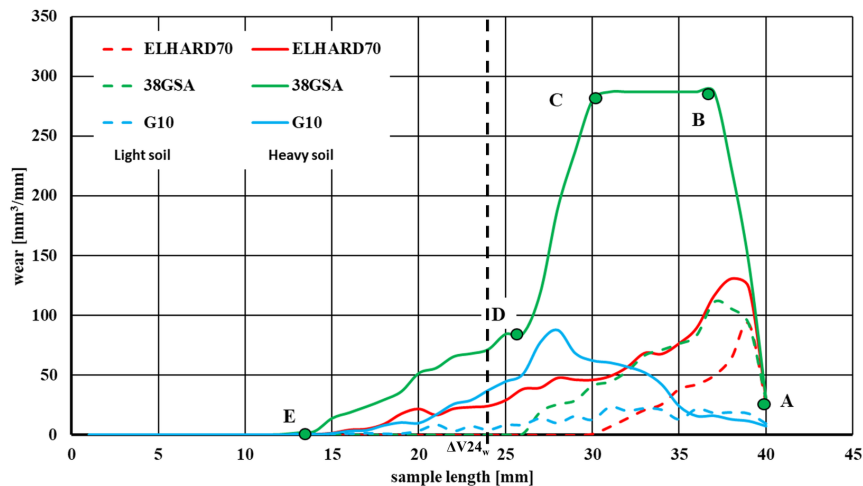


Fig. 16. Local volumes of the worn material

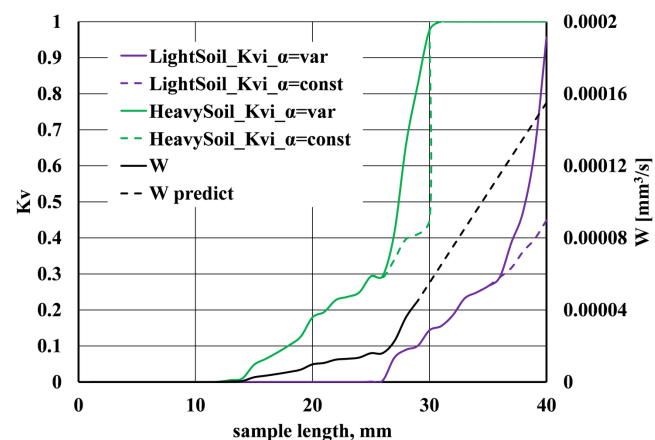


Fig. 17. The relationship between the volumetric wear coefficient K_v and the abrasive grain sliding trajectory

It was also presented how the proposed K_{vi} coefficient can be used to analyze the dependence of wear in relation to the shape of the surface. If the actual sliding trajectory of soil particles along the surface is neglected, assuming $\alpha = \text{const} = 0^\circ$, local wear will be characterized in Fig. 17 by curves marked with broken lines. The characteristics will then be linear. In fact, $\alpha = \text{var}$ (in Fig. 17 this corresponds to the curves drawn with solid lines). The previously noted breakthrough

in the characteristics therefore indicates a change/increase in the slip path along the wedge surface $\alpha < 90^\circ$. For samples from 38GSA material tested in heavy soil, at the length $x = 25.5$ mm, there is a transition to the working surface of the wedge. This explains the sudden increase in K_{vi} .

Table 5 summarises the examples of volumes of each chisel, determined between the initial part of the chisel and the 84 mm cross section (the last section which included all the chisels) and between the 84 mm cross section and the final end of a particular chisel. As for the chisel which performed the ploughing over an area of 6 ha, a negligible volume value was noted virtually above the 84 mm cross section. The greatest volumes were noted for the chisels mounted on the fourth body, with these volumes being more than five times smaller for the chisel, which performed work over an area of 6 ha than those for a new chisel.

Based on the courses of the curves depicting the chisel wear, summarised in Fig. 18, it can be concluded that the wear intensity is strictly determined by the mounting holder location and the amount of work performed. What can be seen is the different wear course for chisels mounted on the first plough body.

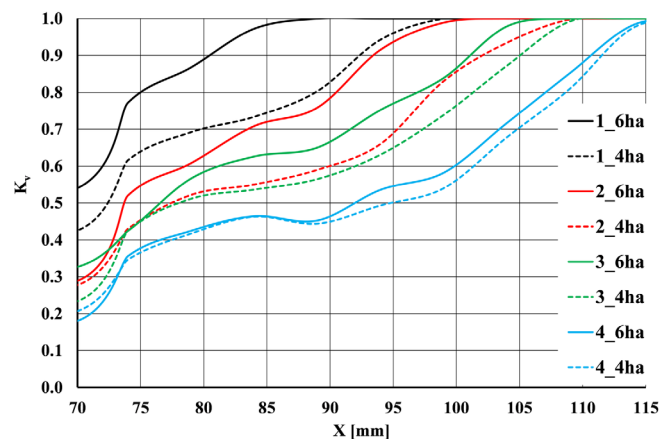


Fig. 18. Characteristics of local volumetric wear of chisels (Fig. 1).

As regards the chisels mounted on the first body which performed work over an area of 6 ha, total wear was found at a distance of 89 mm from the clamping edge. In the analysed area (above the distance

Table 5. Results of the chisel wear determination by the volumetric and mass methods

Chisel No	Entire chisel volume V [mm ³]	Volume below the 84 mm cross section	Volume above the 84 mm cross section
		$\sum_0^{84} V_{iw}$ [mm ³]	$\sum_{85}^l V_{iw}$ [mm ³]
New	132064	66189.6	65874.8
1 - 6 ha	41235	41104.5	130.593
1 - 4 ha	45427.4	42946.3	2481.13
2 - 6 ha	50784.8	47785.5	2999.3
2 - 4 ha	53985.8	46331.8	7653.95
3 - 6 ha	56049.7	50546.5	5503.26
3 - 4 ha	60663.4	52726.2	7937.23
4 - 6 ha	66698.1	55188.2	11509.9
4 - 4 ha	67105.5	54970.7	12134.8

X = 70 mm), the chisel wear exceeded 50% of the volume of a nominal operating part, and from the distance X = 75 mm, even 80% of the volume. The chisel also mounted on the first plough body, which performed work equivalent to 4 ha, exhibited less wear intensity, which is associated with the smaller amount of work performed. A characteristic of the chisels mounted on the first body was the steep wear increase (section C-B), which is due to the wear of the back part of the chisel. The chisel mounted on the second plough body (6 ha) exhibited a very similar course of wear. Despite having performed 50% more work, the wear was slightly lower. Having compared the wear of chisels mounted on the first and second plough body, it can be concluded that for the latter, their wear is approx. 20% less. There was significantly less wear for the chisels mounted on the third and fourth plough body. At a distance of 70 mm from the clamping edge, the chisel mounted on the third body was worn by over 30% after performing the work over 6 ha, and by approx. 25% after performing the work over 4 ha. The difference in wear between chisels performing different amounts of work contributes to an increase in wear by only a maximum of 5%. However, despite the different nature of the wear of individual chisels, an analysis of the wear on each chisel helps to distinguish the same characteristic areas of wear. For the purposes of analysis, wear intensity can be regarded as the slope of a curve. For each chisel, a section with the highest wear intensity value is clearly visible. This is a section located near the cutting edge, section A-B (marked in the figure for chisel 4). The intensity value is similar for almost every chisel. In the B-C section for chisel 4, a range can be distinguished in which the intensity of wear was the lowest. This was particularly true for chisels 3 and 4. On the other hand, within the C-D area, a moderate wear area with a higher intensity was distinguished. The D-E area was also characterised by a high value of wear intensity. However, in this area, the value was due to the characteristic shape of chisels in this area (excess material in new parts on the operating surface of the chisel). There is also a transition zone for the part's surfaces that are less susceptible to wear, and these are the sections running north to east. As the duration of wear processes increases, the transition zone decreases, which is evident in chisels 1 and 2.

5. Conclusions

The paper presents the use of modern, non-contact methods of assessing the wear of working elements processing soil abrasive mass. To test the wear, an original method was used that uses the discretization of the tested space based on the 3D scanning technology and the examination of the surface condition with a microscope.

The three-dimensional surface defect models developed in the article, obtained on the basis of 3D scanning with an accuracy of

0.02 mm, made it possible to describe the changes in the volumetric wear characteristics of the soil processing elements. New wear characteristics have been proposed that will enable the transition from generalized to local change values. The obtained data on volumetric consumption was presented in the form of the local volumetric consumption coefficient, which is the ratio of the volume of the used element to the nominal volume. The coefficient of local volumetric wear shows the influence of the nominal shape and the slip trajectory of the abrasive particle along the elementary surface on the intensity of wear. The proposed coefficient allows to extend the so far analyzes of the wear of working elements and to supplement the Holm-Archard model commonly used in such issues.

Using the volumetric wear data, it is possible to determine after which time / friction path the total wear of the workpiece occurs. This will facilitate the prediction of the actual working element life and the production of more wear-resistant soil cutting elements.

The credibility of the obtained dependencies is confirmed by the agreement as to the value of mass wear, as well as the results of the application of the proposed method to various friction conditions and materials of working elements of agricultural machines.

On the basis of the scanning results obtained, it can be concluded that the profile of the working element in the case of the tested samples changed significantly. Wear in the abrasive mass with the presented characteristics causes that the cutting edges undergo an intensive change in the thickness of the blade. It is possible to identify zones of moderate and heavy wear.

The developed method of identifying the wear process may be useful for tests related to the assessment of the wear of working elements and the assessment of wear resistance (in terms of geometry, material, conditions of use, etc.), as well as in the search for solutions to reduce wear, focusing on the most critical parts of the working element.

Depending on the type of material and type of soil, it was found different nature of wear. When the materials were being worn in the light soil, the loosely bound abrasive particles, characterised by high freedom of movement, caused scratching and ridging on the friction surface. As the content of loam and dust particles in the soil increases, a different course of wear can be noted. For the material from sintered carbide G10, the surface is slightly scratched and the wear processes are hardly noticeable.

The direction of further research is aimed at finding the relationships between the shape of the surface being worn and the local friction coefficient. Together with the proposed characteristics of local volumetric wear, it will enable further development of modeling of the wear process of soil cutting elements.

References

1. Archard J F, Hirst W. The Wear of Metals under Unlubricated Conditions. Proceedings of the Royal Society of London. Series A. Mathematical and Physical Sciences 1956; 236 (1206): 397–410, <https://doi.org/10.1098/rspa.1956.0144>.
2. Archard J F. Contact and Rubbing of Flat Surfaces. Journal of Applied Physics 1953; 24 (8): 981–988, <https://doi.org/10.1063/1.1721448>.
3. Bayhan Y. Reduction of wear via hardfacing of chisel ploughshare, Tribology International 2006; 39(6): 570–574, <https://doi.org/10.1016/j.triboint.2005.06.005>.
4. Bhakat A K, Mishra A K, Mishra N S. Characterization of wear and metallurgical properties for development of agricultural grade steel suitable in specific soil conditions. Wear 2007; 263 (1–6): 228–233, <https://doi.org/10.1016/j.wear.2006.12.006>.
5. Białobrzeska B, Kostencki P. Abrasive wear characteristics of selected low-alloy boron steels as measured in both field experiments and laboratory tests. Wear 2015; 328–329: 149–159, <https://doi.org/10.1016/j.wear.2015.02.003>.
6. Cucinotta F, Scappaticci L, Sfravara F, Morelli F, Mariani F, Varani M, Mattetti M. On the morphology of the abrasive wear on ploughshares by means of 3D scanning. Biosystems Engineering 2019; 179: 117–125, <https://doi.org/10.1016/j.biosystemseng.2019.01.006>.
7. Er U, Par B. Wear of plowshare components in SAE 950C steel surface hardened by powder boriding. Wear 2006; 261(3): 251–255, <https://doi.org/10.1016/j.wear.2005.10.003>.
8. Hawryluk M, Ziemia J, Zwierzchowski M, Janik M. Analysis of a forging die wear by 3D reverse scanning combined with SEM and hardness tests. Wear 2021; 476: 203749, <https://doi.org/10.1016/j.wear.2021.203749>.
9. Hawryluk M, Ziemia J. Application of the 3D reverse scanning method in the analysis of tool wear and forging defects. Measurement 2018; 128: 204–213, <https://doi.org/10.1016/j.measurement.2018.06.037>.
10. Horvat Z, Filipovic D, Kosutic S, Emert R. Reduction of mouldboard plough share wear by a combination technique of hardfacing. Tribology

- International 2008; 41(8): 778–782, <https://doi.org/10.1016/j.triboint.2008.01.008>.
11. Jacobson S, Hogmark S. Tribologi – Friktion, smörjning och nötning. Liber Utbildning AB, Uppsala, Sweden, 1996, ISBN: 9163415321
 12. Konat Ł, Jasiński R, Białobrzaska B, Szczepański Ł. Analysis of the static and dynamic properties of wear-resistant Hardox 600 steel in the context of its application in working elements. *Materials Science–Poland* 2021; 39(1), <https://doi.org/10.2478/msp-2021-0007>.
 13. Konat Ł, Napiórkowski J, Kołakowski K, Resistance to wear as a function of the microstructure and selected mechanical properties of microalloyed steel with boron. *Tribologia* 2016; 268 (4):101–114, <https://doi.org/10.5604/01.3001.0010.6986>.
 14. Kostencki P, T. Stawicki T. Durability and wear geometry of subsoiler shanks provided with sintered carbide plates. *Tribology International* 2016; 104: 19–35, <https://doi.org/10.1016/j.triboint.2016.08.020>.
 15. Mattetti M, Molari G, Sereni E. Damage evaluation of driving events for agricultural tractors. *Computers and Electronics in Agriculture* 2017; 135: 328–337, <https://doi.org/10.1016/j.compag.2017.01.018>.
 16. Meng H C, Ludema K C. Wear models and predictive equations: their form and content. *Wear* 1995; 181–183 (Part 2): 443–457, [https://doi.org/10.1016/0043-1648\(95\)90158-2](https://doi.org/10.1016/0043-1648(95)90158-2).
 17. Napiórkowski J, Lemecha M, Ł. Konat Ł. Forecasting the Wear of Operating Parts in an Abrasive Soil Mass Using the Holm-Archard Model. *Materials* 2019; 12: 2180, <https://doi.org/10.3390/ma12132180>.
 18. Napiórkowski J, Olejniczak K, Konat Ł. Wear Properties of Nitride-Bonded Silicon Carbide under the Action of an Abrasive Soil Mass. *Materials* 2021; 14(8): 2043, <https://doi.org/10.3390/ma14082043>.
 19. Owsiak Z. Wear of symmetrical wedge-shaped tillage tools. *Soil & Tillage Research* 1997; 43(3): 295–308, [https://doi.org/10.1016/S0167-1987\(97\)00020-2](https://doi.org/10.1016/S0167-1987(97)00020-2).
 20. Quirke S, Scheffler O, Allen C. An evaluation of the wear behaviour of metallic materials subjected to soil abrasion. *Soil & Tillage Research* 1988; 11(1): 27–42, [https://doi.org/10.1016/0167-1987\(88\)90029-3](https://doi.org/10.1016/0167-1987(88)90029-3).
 21. Ranuša M, Gallo J, Vrbka M, Hobza M, Paloušek D, Křupka I, Hartl M. Wear Analysis of Extracted Polyethylene Acetabular Cups Using a 3D Optical Scanner. *Tribology Transactions* 2017; 60 (3): 437–447, <https://doi.org/10.1080/10402004.2016.1176286>.
 22. Stradomski Z. Mikrostruktura w zagadnieniach zużycia staliw trudnościeralnych. Wydawnictwo Politechniki Częstochowskiej, Częstochowa, Poland, 2010, ISBN: 978-83-7193-468-1.
 23. Vrublevskiy O, Napiórkowski J, Gonera J, Tarasiuk W. Numerical wear models for knock-on chisels in real operating conditions. *Journal of Tribology* 2022; 144 (9), <https://doi.org/10.1115/1.4054020>.
 24. Yazici A. Investigation of the reduction of mouldboard ploughshare wear through hot stamping and hardfacing processes. *Turkish Journal of Agriculture and Forestry* 2011: 461–468, <https://doi.org/10.3906/tar-1105-29>.
 25. Ziemba J, Hawryluk M, Rychlik M. Application of 3D Scanning as an Indirect Method to Analyze and Eliminate Errors on the Manufactured Yoke-Type Forgings Forged in SMED Device on Modernized Crank Press. *Materials* 2021; 14 (1): 137, <https://doi.org/10.3390/ma14010137>.